

# Temperature-State Estimation of Lithium-Ion Cells Using a Temperature-Dependent ARX Thermal Model

Ngo Phuong Thanh

Faculty of Electronic Engineering, Thai Nguyen University of Technology, Vietnam

Corresponding Author: Ngo Phuong Thanh

Date of Submission: 08-04-2026

Date of Acceptance: 21-04-2026

## ABSTRACT:

Accurate temperature monitoring is essential for ensuring the safety, durability, and operational reliability of lithium-ion batteries, particularly in electric vehicles and stationary energy storage systems. Direct measurement of the internal cell temperature, however, is difficult in practical battery management systems due to sensor-placement limitations and cost constraints. This study proposes a temperature-state estimation approach based on a linear AutoRegressive with eXogenous input (ARX) model, in which the internal heat-generation signal is used as the driving input of the thermal estimator. Experimental data obtained from Samsung 18650-25R cells under multiple ambient temperature conditions were employed for model identification and validation. The ARX coefficients were first identified at several fixed ambient temperatures and then parameterized as functions of ambient temperature to improve generalization across operating conditions. The estimator was evaluated over the temperature range from 5°C to 45°C. The results show that the proposed approach achieves high estimation accuracy and stable dynamic tracking, with lower estimation errors observed at higher ambient temperatures. Owing to its simple structure, low computational burden, and favorable estimation performance, the proposed method is well suited for real-time implementation in battery management systems.

## KEYWORDS:

Lithium-ion cell; temperature-state estimation; ARX thermal model; battery management system; thermal monitoring

## I. INTRODUCTION

With the continuous advancement of technology, the demand for portable electronic devices such as mobile phones, laptops, and other smart systems has increased significantly. More importantly, growing pressure to reduce greenhouse gas emissions has accelerated the adoption of distributed electrical

energy sources, electric vehicles, and autonomous aerial platforms, thereby creating a substantial need for efficient electrical energy storage systems. In this context, lithium-ion batteries have been widely recognized as one of the most suitable energy-storage technologies for modern electronic devices and stationary energy-storage applications because of their high energy density and superior efficiency. Lithium-ion batteries offer several advantages that remain difficult for other battery technologies to match, including high energy density, long service life, and the absence of memory effect [1]–[3].

At present, lithium-ion batteries are commonly manufactured in the form of compact cells, typically cylindrical or prismatic, in order to reduce mechanical stress within the internal separator layers. Figure 1(a) shows a typical cylindrical 18650 lithium-ion cell rated at 2500 mAh from Samsung, while Fig. 1(b) illustrates the internal structure of a lithium-ion cell manufactured by Tesla.



**Figure 1.** a) Samsung 18650-2500 mAh lithium-ion cell; b) Internal structure of a Tesla lithium-ion cell

The operation of a lithium-ion cell is strongly influenced by the electrochemical processes taking place inside the cell. Because battery cells must satisfy strict requirements in terms of safety and energy efficiency, their operating conditions need to be closely monitored. In this context, estimating the internal operating states of the battery and maintaining them within safe limits are of critical importance. Two key operating states are the state of charge (SoC) and the state of temperature (SoT). The temperature state describes the thermal distribution inside the battery, including both heat-generation and heat-dissipation processes during normal operation.

Heat dissipation in a battery cell generally involves conduction, convection, and thermal radiation. Among these mechanisms, thermal radiation is often considered negligible because of the thermal characteristics of lithium-ion cells. In battery packs, internal thermal distribution must be carefully monitored and controlled, since temperature nonuniformity among cells can lead to rapid performance degradation. For thermal monitoring and control purposes, the temperature state is commonly characterized by three quantities: core temperature, average internal temperature, and surface temperature. Accordingly, the thermal dynamics of a battery cell can be described by the following equation:

$$\rho C_p \frac{dT}{dt} = \dot{q}_{cell} + hA(T_{amb} - T)$$

$$\dot{q}_{cell} = I(V_{OC} - V_b) + I \left( T \frac{\partial V_{OC}}{\partial T} \right) \quad (1)$$

where  $\rho$  and  $C_p$  are the density and specific heat capacity, respectively,  $\dot{q}_{cell}$  denotes the internal heat-generation rate,  $h$  is the convective heat-transfer coefficient,  $A$  is the heat-exchange area, and  $T_{amb}$  and  $T$  are the ambient and cell temperatures. Lithium-ion cells are designed to operate only within manufacturer-specified temperature and voltage limits. Exceeding these limits may not only reduce electrochemical performance but also create serious safety hazards, including thermal runaway under high-temperature conditions. At elevated temperature, decomposition of the solid electrolyte interphase and gas generation may occur, increasing the risk of short circuit and explosion. At low temperature, metallic lithium may deposit on the negative electrode, leading to lithium plating, performance deterioration, and accelerated aging.

Prolonged operation under such conditions ultimately accelerates battery aging, and excessively low temperature may even damage the negative electrode. Although battery manufacturers have developed lithium-ion cells with improved thermal stability, these cells may still experience thermal instability and temperature-induced degradation when subjected to high-power operating conditions, such as rapid acceleration and deceleration in electric vehicles, and especially during fast charging [4]–[6]. If thermal management is inadequate, the battery may exceed its safe operating limits and enter an

overheated state, triggering strong exothermic reactions, toxic gas release, severe electrolyte combustion, and ultimately thermal runaway. Once initiated, this phenomenon may propagate from one cell to neighboring cells, leading to fire or explosion [7], [8].

To prevent these hazardous events during operation, a battery management system (BMS) is employed to monitor battery variables and supervise battery operation. However, owing to the limitations of available measurement systems, it is not always possible to directly measure all internal states of every battery cell, particularly the temperature state (SoT). Therefore, a battery model capable of accurately predicting both thermal and electrical quantities is required for implementation in a BMS. The development of accurate models for estimating the temperature state and relevant battery parameters has thus become increasingly important for enabling effective thermal-management strategies and preventing thermal faults in practical battery systems [9], [10].

For thermal modeling, parameters such as specific heat capacity and convective heat-transfer coefficient are often difficult to identify accurately, especially when measurement data are affected by noise. In this context, the ARX model offers several advantages. By incorporating input information explicitly, it can better capture the relationship between the driving signal and the internal temperature of the cell, thereby improving modeling accuracy. In addition, the ARX structure is linear, which simplifies parameter estimation through methods such as least squares.

Compared with nonlinear approaches, including artificial neural networks (ANN) and nonlinear autoregressive exogenous (NARX) models, ARX requires lower computational effort and is therefore more suitable for real-time applications where rapid model updating is required. When the numbers of poles and zeros are selected appropriately, the ARX model can achieve a good balance between accuracy and robustness while preserving numerical stability [11], [12].

## II. ARX MODEL FOR TEMPERATURE ESTIMATION

This study uses Samsung 18650 cells with a nominal capacity of 2500 mAh, as described in Fig. 1. In practice, the surface temperature of a battery cell

can be measured using sensors attached to the cell surface. However, the core temperature can only be measured using specialized laboratory

instrumentation, typically by drilling into the cell and embedding an internal sensor, which is not feasible for commercial batteries.

For thermal modeling, it is well known that thermal parameters are often difficult to determine accurately. In particular, battery heat generation is governed by complex electrochemical reactions, while thermal parameters are strongly affected by measurement noise and operating disturbances. A highly accurate thermal description would generally require solving multiple partial differential equations with respect to both temporal and spatial thermal

### 1. ARX Model Structure

The ARX model adopted in this study is shown in Fig. 2. In this framework, the electrical submodel captures the relationship among the state of charge

distributions inside the cell, which significantly increases computational burden and limits practical applicability [11], [12].

For this reason, an ARX-based thermal model is proposed in this work. Experimental data were collected and tested at ambient temperatures of 5°C, 15°C, 25°C, 35°C, and 45°C. By considering multiple temperature operating points, the variation of the thermal-model parameters with respect to ambient temperature can be captured more accurately.

(SoC), the heat-generation rate  $\dot{q}_{cell}$ , the cell current  $I_{cell}$ , and the cell temperature  $T_{cell}$ , as described in [5], [6].

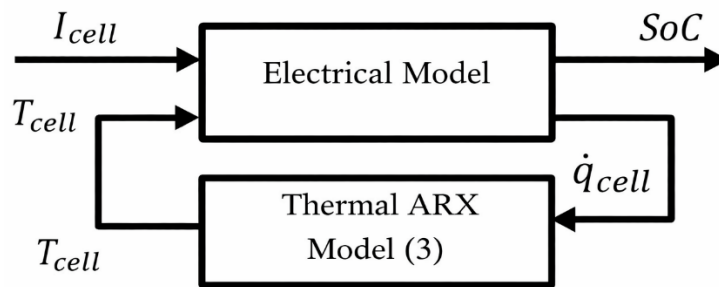


Figure 2. ARX model structure

According to the internal cell-temperature expression in (1), it can be seen that parameters such as the density  $\rho$ , the specific heat capacity  $C_p$ , and the convective heat-transfer coefficient  $h$  are difficult to determine accurately. For this reason, the thermal behavior is represented here by an ARX-structured model, expressed as follows in (2):

$$A(z)T_{cell}(k) = B(z)\dot{q}_{cell}(k) + e(k) \quad (2)$$

where the polynomials  $A(z)$  and  $B(z)$  are given by (3):

$$A(z) = 1 + a_1z^{(-1)} + \dots + a_{(n_a)}z^{(-n_a)}$$

$$B(z) = b_1 + b_2z^{(-1)} + \dots + b_{(n_b)}z^{(-n_b-1)} \quad (3)$$

where  $e(k)$  is a white-noise term affecting the model output,  $z$  is the delay operator, and  $n_a$  and  $n_b$  denote the numbers of poles and zeros of the model, respectively. The coefficients  $a_1, \dots, a_{n_a}$  are

those of the polynomial  $A(z)$ , while  $b_1, \dots, b_{n_b}$  are the coefficients of the polynomial  $B(z)$ . The coefficients of both  $A(z)$  and  $B(z)$  are functions of the ambient temperature.

The numbers of poles and zeros directly influence the data-fitting capability of the ARX model. If too few poles and zeros are selected, the model may not be sufficiently flexible to represent the actual thermal dynamics of the process. On the other hand, if too many poles and zeros are used, the model may become overfitted to the training data, thereby reducing its ability to generalize to unseen data. Therefore, the model structure must be chosen carefully so as to achieve a suitable balance between accuracy and robustness in thermal-process representation.

## 2. Identification of ARX Thermal-Model Parameters

### 2.1. Identification Data

The data used for thermal-model identification were collected at fixed ambient temperatures of

$$T_{amb}=[5^{\circ}\text{C},15^{\circ}\text{C},25^{\circ}\text{C},35^{\circ}\text{C},45^{\circ}\text{C}]$$

The recorded variables include cell temperature, cell current, cell voltage, discharged capacity, charged capacity, and internal cell temperature. These datasets are presented in Figs. 3–7.

Experimental data,  $T_s = 0.08 \text{ s}$

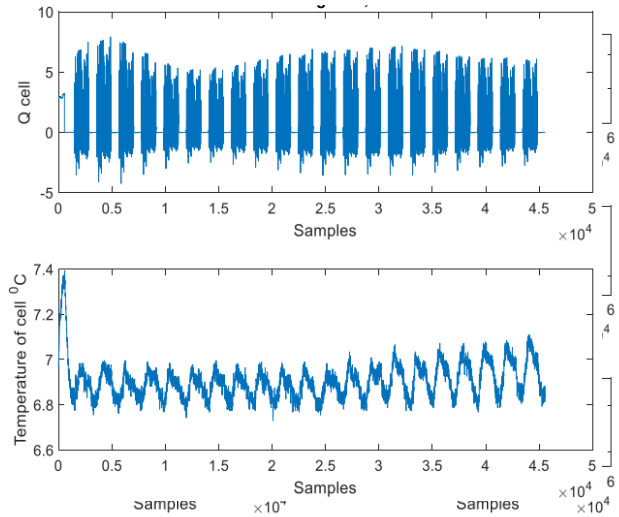


Figure 3. Thermal-model identification data at an ambient temperature of  $5^{\circ}\text{C}$

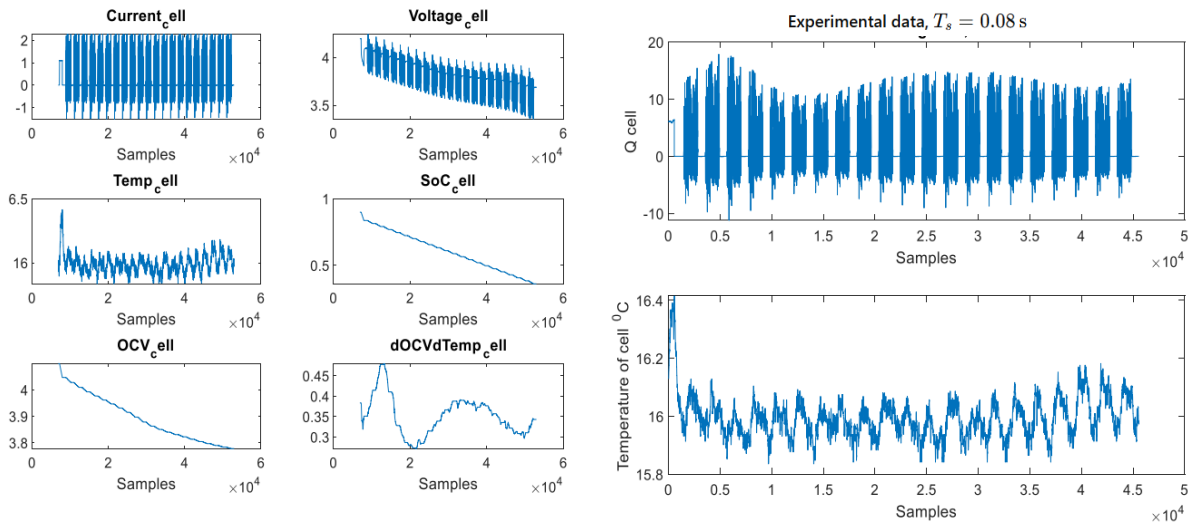


Figure 4. Thermal-model identification data at an ambient temperature of  $15^{\circ}\text{C}$

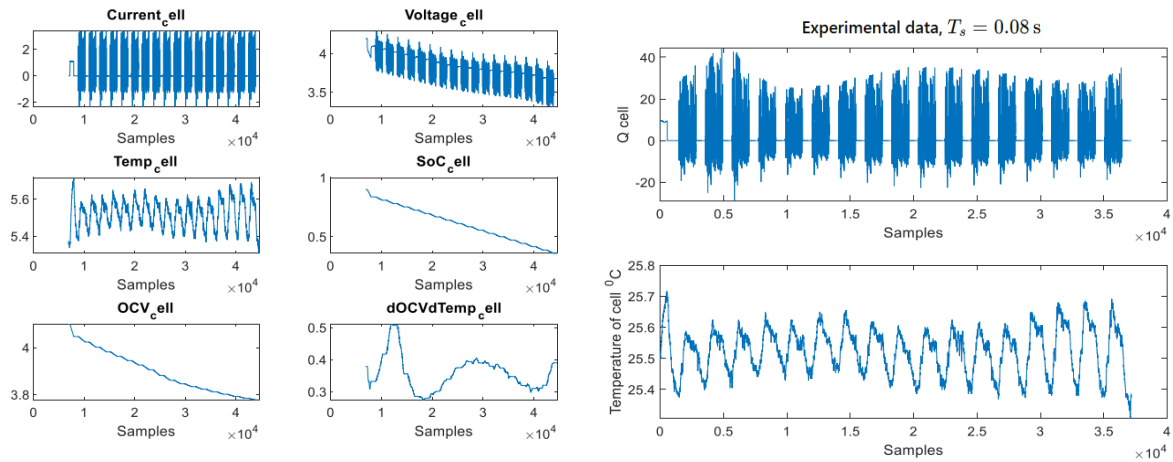


Figure 5. Thermal-model identification data at an ambient temperature of 25°C

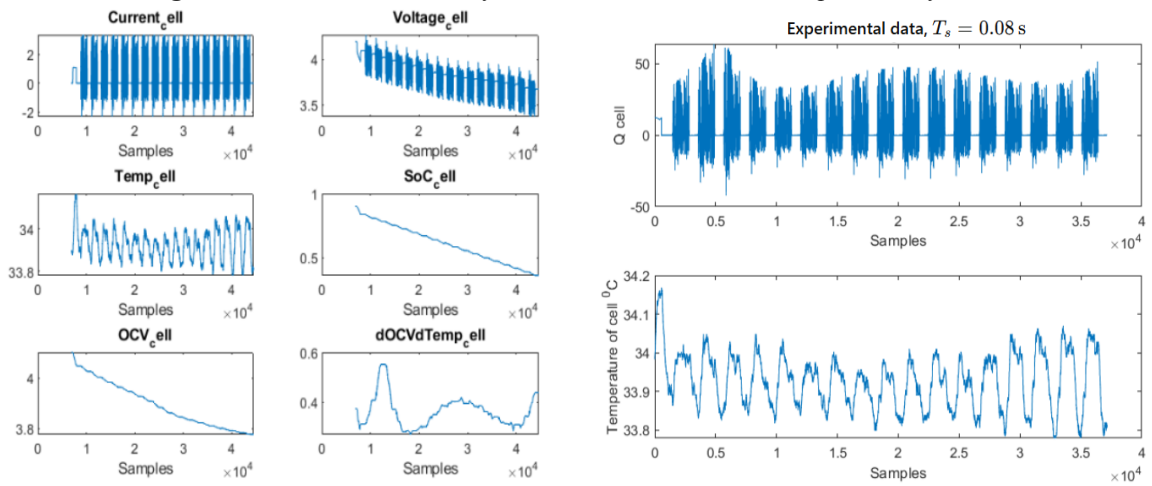


Figure 6. Thermal-model identification data at an ambient temperature of 35°C

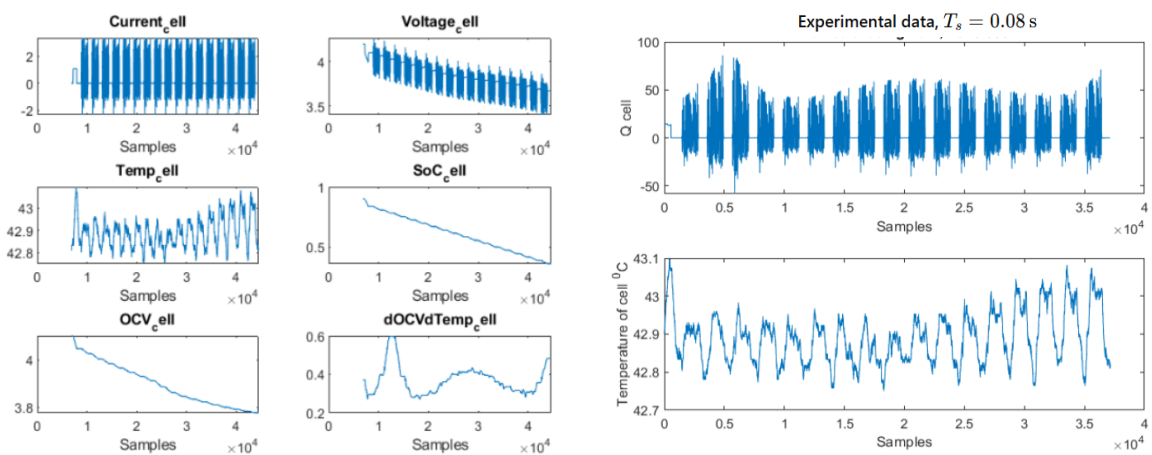


Figure 7. Thermal-model identification data at an ambient temperature of 45°C

### 2.2. Identification Algorithm

From the experimental data, the cell state of charge, the open-circuit voltage  $V_{OC}^i(k)$ , and the temperature coefficient  $\partial V_{OC}^i / \partial T_{cell}^i$  at the  $i$ -th test temperature can be determined. The heat-generation rate  $\dot{q}_{cell}^i$  is then computed using (4):

$$\dot{q}_{cell}^i(k) = u^i(k)(V_{OC}^i(k) - V_{cell}^i(k)) + u^i(k) \left( T_{cell}^i(k) \frac{\partial V_{OC}^i}{\partial T_{cell}^i} \right) \quad (4)$$

Based on  $\dot{q}_{cell}^i(k)$  and  $T_{cell}^i(k)$ , the ARX thermal model corresponding to five different ambient-temperature conditions ( $i = 1, 2, \dots, 5$ ) is written as  $A^i(z)T_{cell}^i(k) = B^i(z)\dot{q}_{cell}^i(k) + e(k)$ ,  $i = 1, 2, \dots, 5$  (5) where the polynomials  $A^i(z)$  and  $B^i(z)$  are defined by (6):

$$A^i(z) = 1 + a_1^i z^{-1} + \dots + a_{n_a}^i z^{-n_a}$$

$$B^i(z) = b_1^i + b_2^i z^{-1} + \dots + b_{n_b}^i z^{-n_b+1} \quad (6)$$

where  $e(k)$  denotes a white-noise disturbance acting on the model output,  $z$  is the delay operator, and  $n_a$  and  $n_b$  are the numbers of poles and zeros, respectively. The coefficients  $a_1^i, \dots, a_{n_a}^i$  and  $b_1^i, \dots, b_{n_b}^i$  correspond to the polynomials  $A^i(z)$  and  $B^i(z)$ . The ARX parameters are identified using the least-squares method or MATLAB's system identification toolbox.

After identifying the coefficients  $a_1^i, \dots, a_{n_a}^i$  and  $b_1^i, \dots, b_{n_b}^i$ , the ambient-temperature-dependent coefficients  $a_1(T_{amb}), \dots, a_{n_a}(T_{amb})$  and  $b_1(T_{amb}), \dots, b_{n_b}(T_{amb})$  are obtained by polynomial fitting using polyfit with polynomial order  $n = 5$ . The internal cell temperature is then estimated by

$$A(z)T_{cell}(k) = B(z)\dot{q}_{cell}(k) + e(k) \quad (7)$$

where the polynomials  $A(z)$  and  $B(z)$  are given by

$$A(z) = 1 + a_1(T_{amb})z^{-1} + \dots + a_{n_a}(T_{amb})z^{-n_a}$$

$$B(z) = b_1(T_{amb}) + b_2(T_{amb})z^{-1} + \dots + b_{n_b}(T_{amb})z^{-n_b+1} \quad (8)$$

More specifically, for each ambient temperature  $T_{amb}(i)$ , the procedure for determining the polynomials  $A^i(z)$  and  $B^i(z)$  is as follows:

From the data  $\dot{q}_{cell}^i(k)$  and  $T_{cell}^i(k)$ , compute the deviations of the input and output data:

$$\Delta \dot{q}_{cell}^i(k) = \dot{q}_{cell}^i(k) - \text{mean}(\dot{q}_{cell}^i(k))$$

$$\Delta T_{cell}^i(k) = T_{cell}^i(k) - \text{mean}(T_{cell}^i(k)) \quad (9)$$

Let the lengths of the datasets  $\Delta \dot{q}_{cell}^i(k)$  and  $\Delta T_{cell}^i(k)$  be denoted by  $l_{data}$ . These datasets are divided into two equal parts: one part is used for parameter estimation and the other for model validation.

The ARX model structure is chosen with an autoregressive order of 5, an input order of 5, and an input delay of  $nk = 2$ . Because the thermal response of the cell to changes in  $\Delta \dot{q}_{cell}^i$  is slower, the delay is selected as  $nk = 2$ .

The model parameters are identified using the least-squares method.

Model accuracy is assessed using the fit percentage, the final prediction error (FPE), and the mean squared error (MSE).

### 2.3. Results of Thermal-Model Identification

The identified coefficients of the polynomials  $A^i(z)$  and  $B^i(z)$  for different ambient-temperature conditions are summarized in Table 1. The corresponding ambient-temperature-dependent coefficients of the polynomials  $A(z)$  and  $B(z)$  are presented in Fig. 8.

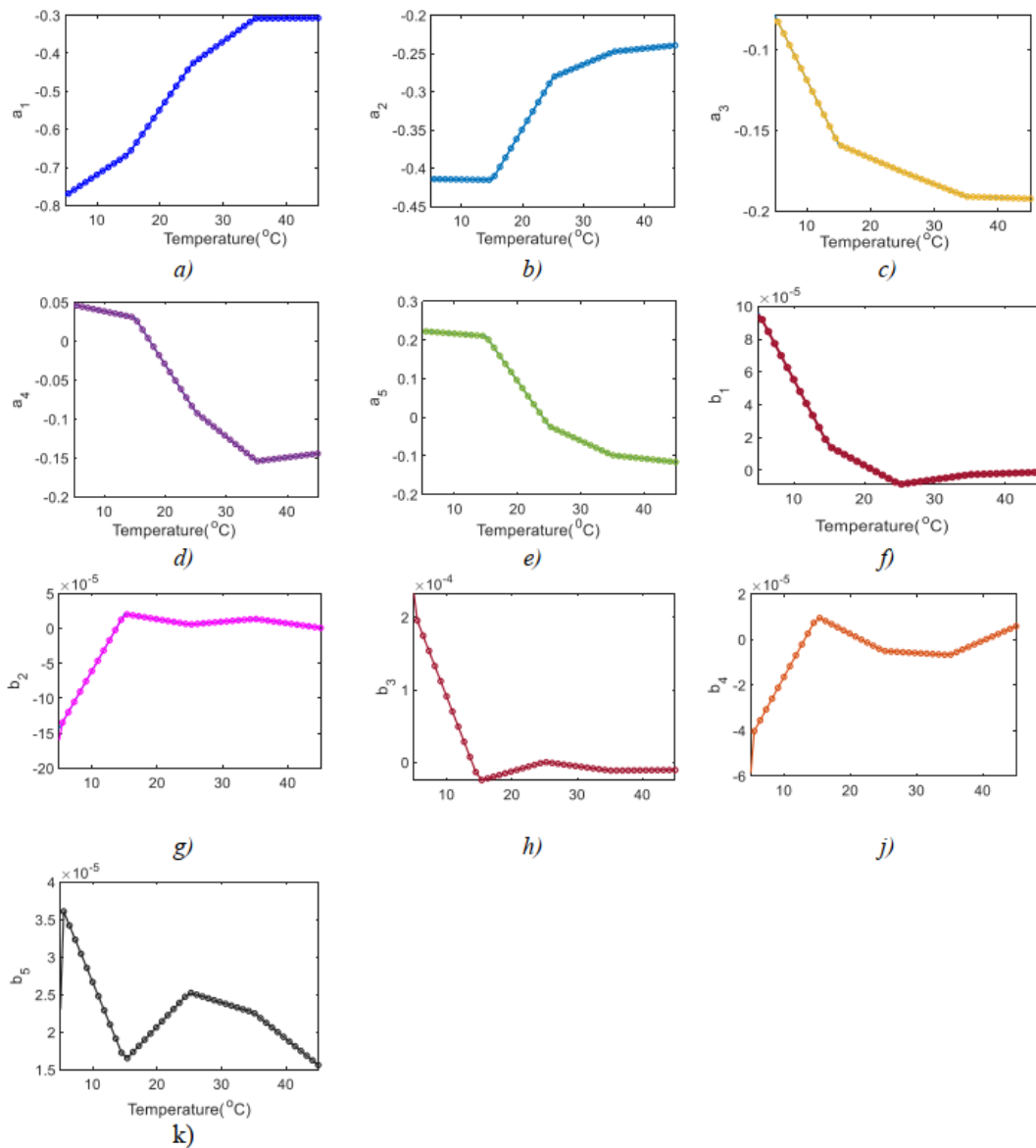


Figure 8. Coefficients of the polynomials  $A(z)$  and  $B(z)$  as functions of ambient temperature

$T_{amb}(t)$	$A^i(z)$ và $B^i(z)$						Fit (%)	FPE	MSE
	$z^{-6}$	$z^{-5}$	$z^{-4}$	$z^{-3}$	$z^{-2}$	$z^{-1}$			
$T_{amb}(1)$ = 5°C	$A^4(z)$	0,2231	0,04667	- 0,07867	- 0,4141	- 0,774	94,82	1,977e-05	1,975e-05
$T_{amb}(2)$ = 15°C	$B^4(z)$	3,718e-05	- 4,301e-05	0,0002074	- 0,0001429	9,607e-05	95,07	1,455e-05	1,453e-05
$T_{amb}(3)$ = 25°C	$A^5(z)$		0,21	0,0305	- 0,1588	- 0,4154	- 0,6644		
$T_{amb}(4)$ = 35°C	$B^5(z)$	1,619e-05	1,001e-05	- 2,552e-05	2,082e-05	1,472e-05	- 0,4285	94,85	1,112e-05
$T_{amb}(5)$ = 45°C	$A^6(z)$		- 0,02322	- 0,09088	- 0,1756	- 0,2808			
	$B^6(z)$	2,531e-05	- 5,082e-06	4,146e-07	5,715e-06	- 8,569e-06	- 0,3084	94,86	1,173e-05
	$A^7(z)$		- 0,09833	- 0,1539	- 0,191	- 0,2475	- 0,3072	93,44	1,492e-05
	$B^7(z)$	2,26e-05	- 6,848e-06	- 1,141e-05	1,371e-05	- 2,581e-06			1,489e-05
	$A^8(z)$		- 0,1158	- 0,1443	- 0,1923	- 0,2394			
	$B^8(z)$	1,563e-05	5,787e-06	- 1,066e-05	8,703e-07	- 1,147e-06			

Table 1. Coefficients of the polynomials  $A^i(z)$  and  $B^i(z)$  for different ambient temperatures

### 3. Temperature-State Estimation Results (SoT)

#### 3.1. Structure of the SoT Estimator

The state of temperature (SoT) is estimated using the following expression:

$$\begin{aligned} \hat{T}_{cell}(k) = & b_1(T_{amb})\hat{q}_{cell}(k-2) + b_2(T_{amb})\hat{q}_{cell}(k-3) \\ & + b_3(T_{amb})\hat{q}_{cell}(k-4) + b_4(T_{amb})\hat{q}_{cell}(k-5) \\ & + b_5(T_{amb})\hat{q}_{cell}(k-6) - a_1(T_{amb})\hat{T}_{cell}(k-1) \\ & - a_2(T_{amb})\hat{T}_{cell}(k-2) - a_3(T_{amb})\hat{T}_{cell}(k-3) \\ & - a_4(T_{amb})\hat{T}_{cell}(k-4) - a_5(T_{amb})\hat{T}_{cell}(k-5) \end{aligned} \quad (10)$$

where the coefficients  $b_j(T_{amb})$  and  $a_j(T_{amb})$  are identified from the temperature-dependent polynomial fits shown in Fig. 8, and  $\hat{q}_{cell}$  is obtained from the experimental measurements.

#### 3.2. SoT Estimation Results

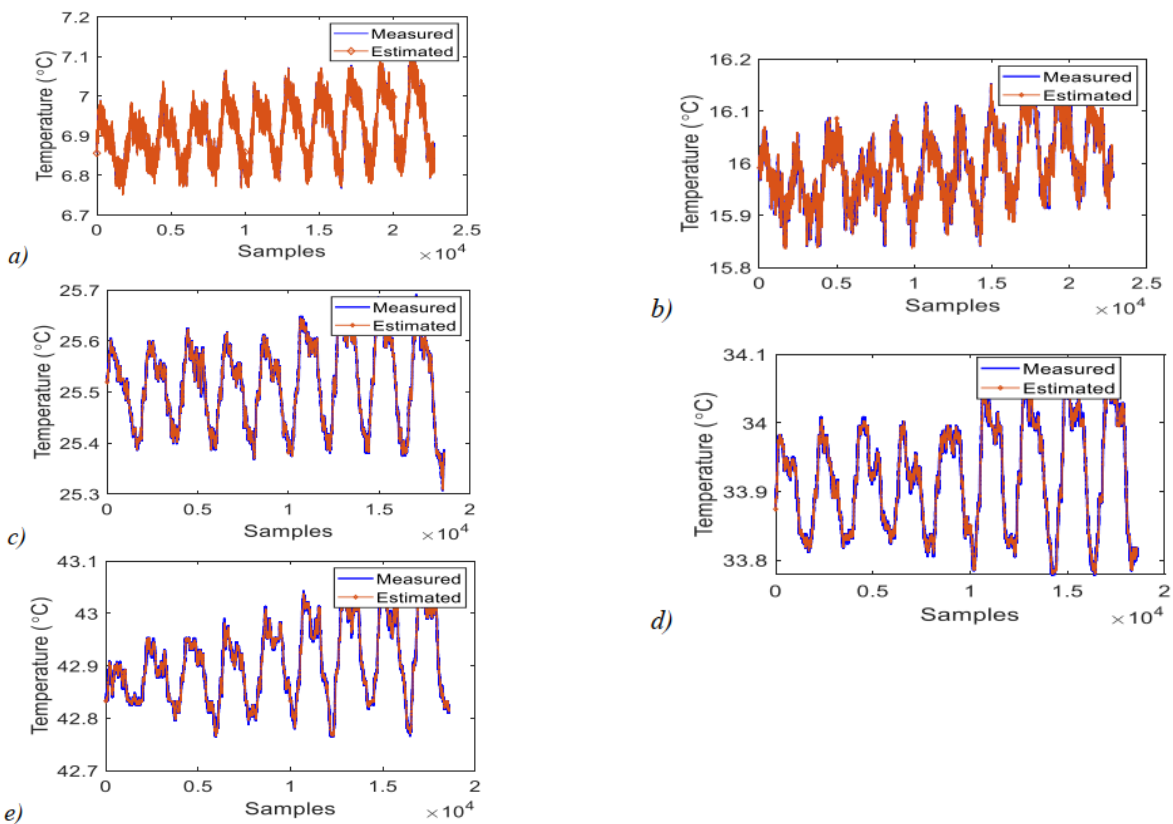


Figure 9. SoT estimation results at the test temperatures: a) 5°C, b) 15°C, c) 25°C, d) 35°C, e) 45°C

Chỉ tiêu	5°C	15°C	25°C	35°C	45°C
MSE	3,4349e-04	1,6562e-04	6,2880e-05	3,8890e-05	4,3619e-05
RMSE	0,0185	0,0129	0,0079	0,0062	0,0066
MAPE (%)	0,2207	0,0624	0,0230	0,0133	0,0111

Table 2. Error metrics for SoT estimation

The SoT estimation results under the experimental scenarios corresponding to different cell temperatures are shown in Fig. 9. The error metrics for SoT estimation, including MSE, RMSE, and MAPE, are reported in Table 2.

According to Table 2, the SoT estimation error decreases as the ambient temperature increases from 5°C to 45°C. In particular, the MAPE decreases from 0.2207% at 5°C to 0.0111% at 45°C. This indicates

### III. CONCLUSION

This paper has presented a temperature-state estimation method for lithium-ion battery cells using a linear ARX model. By using the internally dissipated power as the model input, the proposed approach is able to represent the internal thermal dynamics of the battery accurately without requiring direct identification of complex thermal parameters. Experimental results and error-evaluation metrics show that the proposed method achieves high estimation accuracy over a wide temperature range.

### IV. ACKNOWLEDGEMENT

The author would like to thank Thai Nguyen University of Technology (TNUT), Vietnam for the support. (<http://www.tnut.edu.vn/>).

### REFERENCES

- [1]. H. Bajolle, M. Lagadic, and N. Louvet, "The future of lithium-ion batteries: Exploring expert conceptions, market trends, and price scenarios," *Energy Research & Social Science*, vol. 93, 2022, Art. no. 102850.
- [2]. K. Smith and C.-Y. Wang, "Power and thermal characterization of a lithium-ion battery pack for hybrid electric vehicles," *Journal of Power Sources*, vol. 160, no. 1, pp. 662-673, 2006.
- [3]. F. Degen *et al.*, "Energy consumption of current and future production of lithium-ion and post lithium-ion battery cells," *Nature Energy*, vol. 8, no. 11, pp. 1284-1295, 2023.
- [4]. S. Yang, C. Deng, Y. Zhang, and Y. He, "State of Charge Estimation for Lithium-Ion Battery with a Temperature-Compensated 10.3390/en10101560
- [5]. S. Huang, K. Tseng, J. Liang, C. Chang, and M. G. Pecht, "An Online SOC and SOH Estimation Model for Lithium-Ion Batteries," *Energies*, vol. 10, no. 4, 2017, Art. no. 512, doi: 10.3390/en10040512.
- [6]. S. Barcellona, S. Colnago, P. Montrasio, and L. Piegari, "Integrated Electro-Thermal Model for Li-Ion Battery Packs," *Electronics*,

that the proposed model achieves higher estimation accuracy at elevated temperatures. In other words, the SoT estimator performs more effectively and accurately under higher ambient-temperature conditions. One possible explanation is that, at higher temperatures, the identified coefficients of the polynomials  $A(z)$  and  $B(z)$  can be determined more accurately, while the ratio of measurement noise to the temperature magnitude becomes smaller.

Owing to its simple structure, computational efficiency, and high stability, the ARX-based approach is well suited for implementation in practical battery management systems. In future work, the model may be extended to enable simultaneous estimation of SoT and SoC, or integrated with nonlinear models to further improve accuracy under more demanding operating conditions.

- vol. 11, no. 10, 2022, Art. no. 1537, doi: 10.3390/electronics11101537.
- [7]. P. Van den Bossche, N. Omar, M A. Sakka, *et al.*, "The challenge of phev battery design and the opportunities of electrothermal modeling," *Lithium-Ion Batteries*, vol. 2014, pp. 249-271, 2014
- [8]. J. Newman and C. R. Pals, "Thermal Modeling of the Lithium/Polymer Battery I. Discharge Behavior of a Single Cell," *Journal of the Electrochemical Society*, vol. 142, no. 10, pp. 3274-3281, 1995.
- [9]. C. R. Pals and J. Newman, "Thermal Modeling of the Lithium/Polymer Battery II. Temperature Profiles in a Cell Stack," *Journal of the Electrochemical Society*, vol. 142, no.10, pp.3282-3288, 1995.
- [10]. W. B. Gu and C. Y. Wang, "Thermal-Electrochemical Modeling of Battery Systems," *J. Electrochem. Soc.*, vol. 147, pp. 2910-2922, 2000.
- [11]. K. Kumaresan, G. Sikha, and R. E. White, "Thermal Model for a Li-Ion Cell," *J. Electrochem. Soc.*, vol. 155, pp. A164-A171, 2008
- [12]. K. Kumaresan, G. Sikha, and R. E. White, "Thermal Model for a Li-Ion Cell," *J. Electrochem. Soc.*, vol. 155, pp. A164-A171, 2008 Model," *Energies*, vol. 10, no. 10, 2017, Art. no. 1560